Colloid and Surface Science
2021; 6(1): 1-7
http://www.sciencepublishinggroup.com/j/css
doi: 10.11648/j.css.20210601.11
ISSN: 2578-9120 (Print); ISSN: 2578-9236 (Online)

Giant Vesicles of Amphiphilic Diblock Copolymer with Branched Side Chains

Eri Yoshida

Department of Applied Chemistry and Life Science, Toyohashi University of Technology, Toyohashi, Japan

Email address:
yoshida.eri.gu@tut.jp

To cite this article:
Eri Yoshida. Giant Vesicles of Amphiphilic Diblock Copolymer with Branched Side Chains. *Colloid and Surface Science*. Vol. 6, No. 1, 2021, pp. 1-7. doi: 10.11648/j.css.20210601.11

Received: September 12, 2021; **Accepted**: October 8, 2021; **Published**: October 15, 2021

Abstract: Biomolecules of lipids and proteins optimize the hydrophobicity to precisely form their three-dimensional structures. The branching of hydrocarbon chains is appropriate for fine-tuning the hydrophobicity of the molecules because it provides a slight reduction in hydrophobicity. This paper describes the morphological changes of vesicles formed by an amphiphilic diblock copolymer supporting branched side chains in the hydrophobic block to elucidate the steric effect of the side chains on the morphology. The vesicles consisting of poly(methacrylic acid)-*block*-poly(isopropyl methacrylate-*random*-methacrylic acid), PMAA-*b*-P(iPMA-*r*-MAA), were obtained by the polymerization-induced self-assembly using the photo-nitroxide mediated controlled/living radical polymerization (photo-NMP) in an aqueous methanol solution (methanol/water=3/1 *v*/*v*). PMAA-*b*-P(iPMA-*r*-MAA) with a very high ratio of the iPMA units produced spherical vesicles. As the iPMA ratio decreased, the vesicles shrank, expanded again, and changed into sheets. The chain length of the hydrophobic block also dominated the morphology. For the high iPMA ratio constant, the copolymers with a short block produced two domains of micron-sized spherical vesicles and unspecific nano-sized particles fused. An increase in the block length changed the nanoparticles into nanospheres, accompanied by an increase in the number of micron-sized spherical vesicles. By further extending the block length, most of the nanospheres grew into micron-sized spherical vesicles. On the other hand, for the low iPMA ratio constant, an increase in the length of the hydrophobic chain changed the unspecific nanoparticles sheets into aggregates with an inverted hexagonal phase reticularly perforated. The PMAA-*b*-P(*n*-propyl methacrylate-*r*-MAA) copolymer produced flexible sheets with a smooth surface without any pores, while PMAA-*b*-P(methyl methacrylate-*r*-MAA) provided rods of laminated sheets. It was found that the formation of the inverted hexagonal phase was due to the steric repulsion of the bulky isopropyl groups in the hydrophobic blocks. These findings indicate that the morphology of the vesicles is manipulated not only by the hydrophobicity of the copolymer, but also by the bulkiness of the branched side chain in the hydrophobic block.

Keywords: Giant Vesicles, Amphiphilic Diblock Copolymer, Morphology Changes, Branched Side Chains, Steric Repulsion, Inverted Hexagonal Phase

1. Introduction

The hydrophobicity of molecules is of significance in living bodies for forming their own three-dimensional structures and taking hydrophobic compounds into them by a hydrophobic interaction. The biomolecules precisely adjust their hydrophobicity by various factors, such as the number of carbons in the hydrocarbon chain, its branching, cyclization, incorporations of double bonds and aromatic groups, and their positions in the chain [1]. All of these factors reduce the hydrophobicity for saturated aliphatic straight-chain hydrocarbons; however, the degree of reduction is not equal [2]. The branching provides a small degree of hydrophobicity reduction, and therefore, it is appropriate for fine-tuning the hydrophobicity. While long-branched hydrocarbon chains are found in fatty acids, especially lipids in bacteria [3, 4], short-branched chains in the essential amino acids of valine, leucine, and isoleucine produce a hydrophobic environment in proteins [5]. Such short-branched hydrocarbons of isopropyl, isobutyl, and secondary butyl groups have also been used in synthetic organic chemistry and supramolecular chemistry for

increasing the hydrophobicity of molecules [6, 7].

Giant vesicles in a micron size are artificial models of biomembrane for cells and organelles due to their similarities in size and structure [8]. The giant polymer vesicles consisting of poly(methacrylic acid)-*block*-poly(methyl methacrylate-*random*-methacrylic acid), PMAA-*b*-P(MMA-*r*-MAA), have produced some significant models; for instance, the villi model with vertically aligned worm-like vesicles [9], the nuclear envelop model using perforated vesicles [10], the membrane protein model for endocytosis employing a polyelectrolyte [11], and the sterol model including the P(MMA-*r*-MAA) segment copolymer [12]. These models are based on similarities to the biomembranes in morphology [13, 14], stimuli-responsive behavior [15], and membrane impermeability [16]. Based on the studies of the polymer vesicles, the isopropyl group was utilized to control the morphology of the vesicles by manipulating the hydrophobicity of the block copolymer [17]. Partial replacement of the MMA units in the hydrophobic P(MMA-*r*-MAA) block with isopropyl methacrylate (iPMA) caused a remarkable change in the vesicle morphology from a sheet into spheres. With the aim of clarifying the steric effect of the isopropyl along with its hydrophobicity, the morphology was investigated for vesicles containing iPMA units in the hydrophobic block. This paper describes the morphology changes in the vesicles consisting of a PMAA-*b*-P(iPMA-*r*-MAA) diblock copolymer.

2. Experimental Work

2.1. Instrumentation

An Ushio UV irradiation system consisting of an optical modulex BA-H502, an illuminator OPM2-502H with a high-illumination lens UI-OP2SL, and a 500W super high-pressure UV lamp USH-500SC2 was used for preparing the polymer vesicles by the polymerization-induced self-assembly through the photo-NMP. ^{1}H NMR measurements were conducted using Jeol ECS400 and ECS500 FT NMR spectrometers. Gel permeation chromatography (GPC) was carried out using a Tosoh GPC-8020 instrument equipped with a DP-8020 dual pump, a CO-8020 column oven, and a RI-8020 refractometer. Two gel columns (Tosoh TSK-GEL α-M) were used with an eluent (*N*,*N*-dimethylformamide containing 30 mM LiBr and 60 mM H_3PO_4) at 40°C. The molecular weight (M_n) and molecular weight distribution (M_w/M_n) were estimated based on PMAA standards. Field emission scanning electron microscopy (FE-SEM) observations were performed using a Hitachi SU8000 scanning electron microscope. The vesicles were dried in air and subjected to the FE-SEM measurements at 1.0 kV without any coating. The morphology and size (D_n) of vesicles were determined by the FE-SEM observation. The size distribution (D_w/D_n) of spherical vesicles was estimated as reported previously [18].

2.2. Materials

Methacrylic acid (MAA) was purified by distillation under reduced pressure. Methyl methacrylate (MMA) and iPMA were passed through a column packed with activated alumina to remove an inhibitor and distilled over calcium hydride. The monomers thus purified were degassed with Ar for 15 min with stirring just before use. 4-Methoxy-2,2,6,6-tetramethylpiperidine-1-oxyl (MTEMPO) was prepared as reported previously [19]. 2,2'-Azobis[2-(2-imidazolin-2-yl)propane] (V-61) and (4-*tert*-butylphenyl)diphenyl-sulfonium triflate (^{t}BuS) were purchased from Wako Pure Chemical Industries and Sigma-Aldrich, respectively, and used as received. Methanol (MeOH) was refluxed over magnesium with a small amount of iodine for several hours and then distilled. Distilled water purchased from Wako Pure Chemical Industries was purified by distillation. Extremely pure N_2 gas with over 99.9995 vol% purity and Ar gas with over 99.999 vol% purity were purchased from Taiyo Nippon Sanso Corporation.

2.3. Polymerization-induced Self-assembly by Photo-NMP. General Procedure

A prepolymer of PMAA end-capped with MTEMPO was prepared as reported previously [13]; V-61 (22.8 mg, 0.0911 mmol), MTEMPO (18 mg, 0.0966 mmol), ^{t}BuS (24.0 mg, 0.0512 mmol), MAA (2.030 g, 23.6 mmol), and MeOH (4 mL) were placed in a 30-mL test tube joined to a high vacuum valve. The contents were degassed several times using a freeze-pump-thaw cycle and then charged with N_2. The photo-NMP was performed at room temperature for 5.5 h with irradiation at 9.3 amperes by a reflective light using a mirror with a 500W super high-pressure UV lamp to prevent any thermal polymerization caused by the direct irradiation [19]. MeOH (11 mL) and distilled water (5 mL) degassed by bubbling Ar for 15 min were added to the product under a flow of Ar. After the product was completely dissolved in the aqueous MeOH solution, part of the mixture (ca. 1 mL) was withdrawn to determine the MAA conversion. The conversion was 77% by ^{1}H NMR. The molecular weight and molecular weight distribution of the PMAA were *Mn*=21,600 and *Mw/Mn*=1.64, respectively, by GPC based on PMAA standards. The solution removed was poured into 50 mL of ether to precipitate the PMAA. The precipitate was collected with a filter and dried in vacuo for several hours to obtain the PMAA end-capped with MTEMPO (68.9 mg).

The solution (9 mL containing 0.0435 mmol of the PMAA and 2.42 mmol of the unreacted MAA based on 77% conversion), iPMA (1.19 g, 9.28 mmol), and MAA (0.533 g, 6.19 mmol) were placed in a 100-mL test tube joined to a high vacuum valve under a flow of Ar. The initial molar ratio of the monomers was iPMA/MAA=0.520/0.480. The contents were degassed several times through a freeze-pump-thaw cycle and finally charged with N_2. The polymerization was performed for 14 h at room temperature with 600 rpm of the stirring speed by irradiation at 9.4 amperes. Part of the resulting dispersion solution (ca. 1 mL) was removed to estimate the monomer conversions. An aqueous MeOH solution (50 mL, MeOH/water=3/1 *v*/*v*) was poured into the dispersion solution to precipitate the aggregates. The

aggregates were cleaned by a repeated sedimentation-redispersion process using the MeOH solution. The resulting vesicles were stored in the MeOH solution.

3. Results and Discussion

The vesicles consisting of PMAA-*b*-P(iPMA-*r*-MAA) were obtained by the polymerization-induced self-assembly using the photo-NMP in an aqueous MeOH solution (MeOH/water=3/1 *v*/*v*) (Table 1 and Figure 1). The molar ratio of units in the hydrophobic P(iPMA-*r*-MAA) block was determined on the basis of the monomer conversions estimated by ^{1}H NMR using the methine proton of the isopropyl for the iPMA conversion and the *trans*-vinyl protons for MAA and iPMA for the MAA conversion (Figure 2). The degree of polymerization (DP) for the hydrophilic PMAA block was calculated using the molecular weight determined by GPC based on PMAA standards, while the DP of the P(iPMA-*r*-MAA) block was estimated by the monomer conversions and the molarity of MTEMPO that determines the molecular weight of the polymer [21, 22]. The GPC profiles of the diblock copolymer and MTEMPO-capped PMAA prepolymer confirmed that no prepolymer was included in the block copolymer (Figure 3).

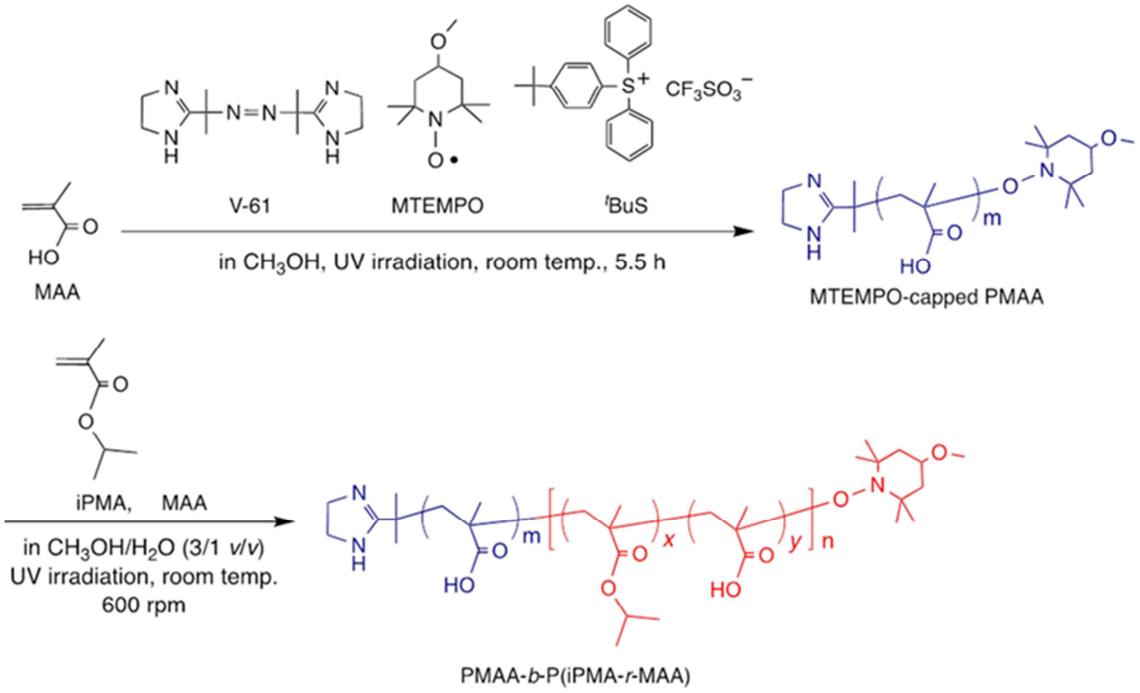

Figure 1. *Synthesis of PMAA-b-P(iPMA-r-MAA).*

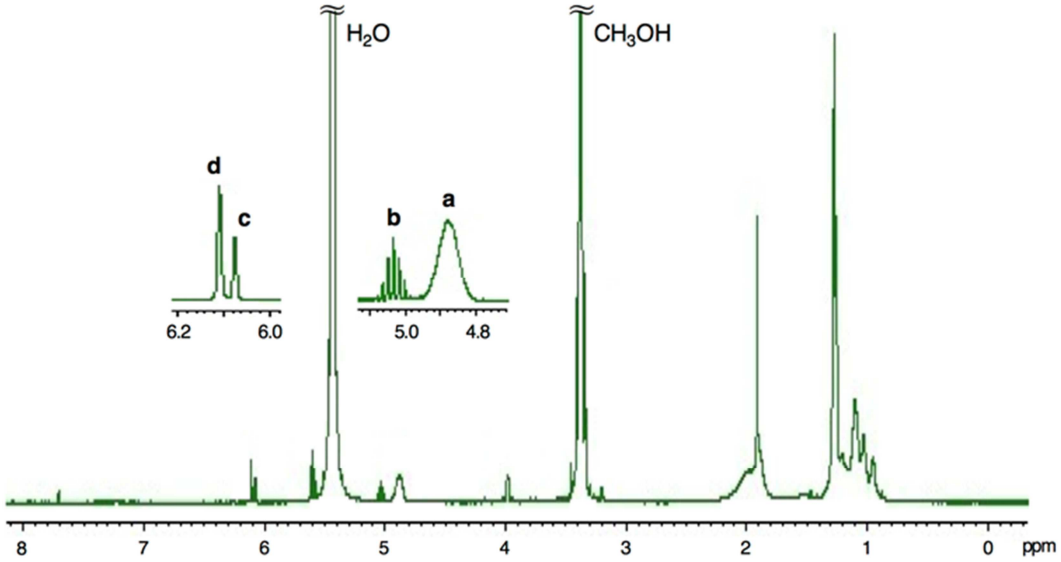

Figure 2. *A ^{1}H NMR spectrum of the dispersion solution obtained by the polymerization-induced self-assembly. The monomer conversions were estimated using the isopropyl methine protons of the polymer (a) and monomer (b) for the iPMA conversion and the trans-vinyl protons of MAA (d) and iPMA (c) for the MAA conversion.*

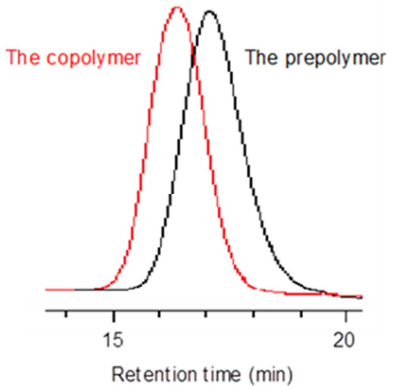

Figure 3. *GPC profiles of the PMAA-b-P(iPMA-r-MAA) diblock copolymer and the MEMPO-capped PMAA prepolymer.*

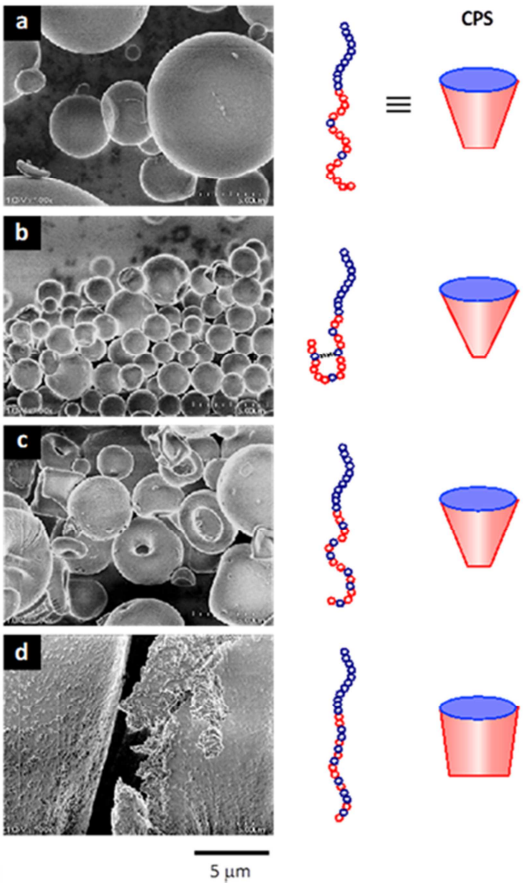

Figure 4. *FE-SEM images of the morphologies by the self-assembly of the diblock copolymers and their critical packing shapes. (a) $PMAA_{211}$-b-$P(iPMA_{0.875}$-r-$MAA_{0.125})_{368}$, (b) $PMAA_{211}$-b-$P(iPMA_{0.755}$-r-$MAA_{0.245})_{306}$, (c) $PMAA_{211}$-b-$P(iPMA_{0.676}$-r-$MAA_{0.324})_{293}$, and (d) $PMAA_{211}$-b-$P(iPMA_{0.583}$-r-$MAA_{0.417})_{298}$.*

FE-SEM observations revealed that the morphology of the vesicles was dependent on the molar ratio of the iPMA units. As shown in Figure 4, the copolymers with a high ratio (x=0.875) of the iPMA units produced spherical vesicles. The size of vesicles decreased as a result of reducing the iPMA ratio to 0.755. Also noted is that a difference between DP=368 and 306 for the hydrophobic blocks is negligible for the morphological change because $PMAA_{212}$-*b*-$P(iPMA_{0.727}$-*r*-$MAA_{0.273})_{360}$ produced spherical vesicles (D_n=1.44 m) as well as $PMAA_{211}$-*b*-$P(iPMA_{0.755}$-*r*-$MAA_{0.245})_{306}$ (D_n=1.87 m), accompanied by a small difference in the vesicle size. In previous studies, for the diblock copolymers containing methacrylates without any bulkiness, the reduction in the molar ratio of the methacrylate units increased the vesicle size because of an increase in the hydrophilicity of the hydrophobic block [23]. The reason for the decrease in the vesicle size by the reduction in the iPMA ratio is that intramolecular hydrogen bonding of the MAA units predominates over steric repulsion of the isopropyl groups that causes shrinking of the hydrophobic phase of the vesicles. A further decrease in the iPMA ratio to 0.676 increased the vesicle size, accompanied by the partial formation of deformed vesicles. More hydrogen bondings within the hydrophobic block encouraged its hydrophilicity to expand the hydrophobic phase. An increase in the hydrophilicity also enhanced the flexibility of the membrane to cause the deformation of the vesicles. The copolymer with a very low iPMA ratio (x=0.583) provided a sheet-like morphology. These morphological changes can also be accounted for by variation in the critical packing shape (CPS) of the copolymer [24]; a truncated cone-like shape at a very high iPMA ratio converts into a sharper shape due to an increase in the hydrogen bonding. The shape reverts to the truncated cone due to an increase in the hydrophilicity by a decrease in the iPMA ratio and finally changes into a cylindrical shape at a still lower iPMA ratio.

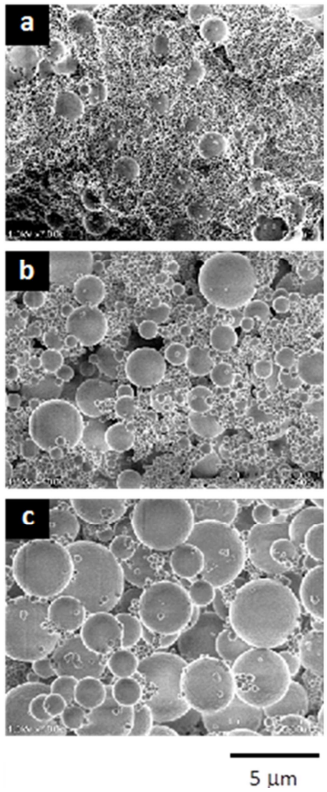

Figure 5. *The effect of the P(iPMA-r-MAA) block length on the morphologies for the high iPMA ratio constant. (a) $PMAA_{216}$-b-$P(iPMA_{0.768}$-r-$MAA_{0.232})_{191}$, (b) $PMAA_{239}$-b-$P(iPMA_{0.807}$-r-$MAA_{0.193})_{255}$, and (c) $PMAA_{244}$-b-$P(iPMA_{0.797}$-r-$MAA_{0.203})_{384}$.*

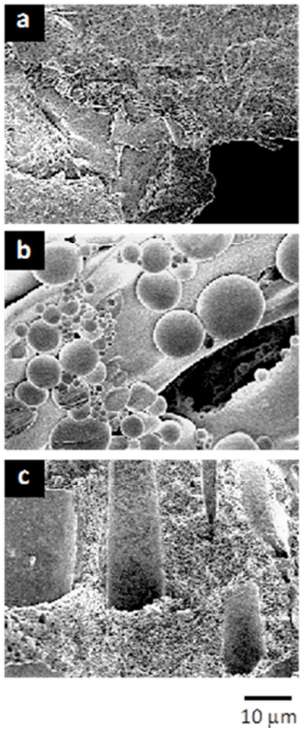

Figure 6. *The effect of the P(iPMA-r-MAA) block length on the morphologies for the low iPMA ratio constant. (a) $PMAA_{244}$-b-$P(iPMA_{0.570}$-r-$MAA_{0.430})_{126}$, (b) $PMAA_{250}$-b-$P(iPMA_{0.554}$-r-$MAA_{0.446})_{251}$, and (c) $PMAA_{248}$-b-$P(iPMA_{0.562}$-r-$MAA_{0.438})_{350}$.*

The chain length of the hydrophobic block also dominated the morphology. Figure 5 shows the variation in the morphology when the P(iPMA-*r*-MAA) block length was increased for the high iPMA ratio constant. The copolymers with a short block produced two domains; one was micron-sized spherical vesicles, and the other was unspecific nano-sized particles fused to each other. A small number of the spherical vesicles was embedded in the nanoparticle domain. An increase in the block length changed the unspecific nanoparticles into nanospheres, accompanied by increasing the number of micron-sized spherical vesicles. The size of the spherical vesicles decreased because the average size included growing nanospheres, which was reflected in the broadening of the size distribution. By further extending the block length, most of the nanospheres grew into micron-sized spherical vesicles. The short block chain has too low a hydrophobicity to associate and forms structurally unstable nanoparticles. On the other hand, the long block chain is hydrophobic enough to self-assemble to produce stable micron-sized spherical vesicles.

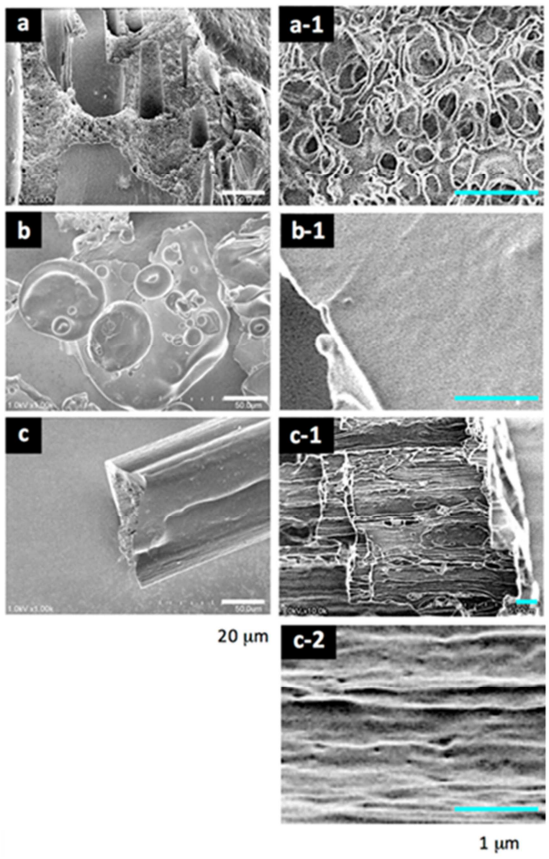

Figure 7. *The morphologies of the diblock copolymers containing different methacrylate units. (a, a-1) $PMAA_{248}$-b-$P(iPMA_{0.562}$-r-$MAA_{0.438})_{350}$, (b, b-1) $PMAA_{233}$-b-$P(nPMA_{0.577}$-r-$MAA_{0.423})_{305}$, and (c, c-1, c-2) $PMAA_{209}$-b-$P(MMA_{0.577}$-r-$MAA_{0.423})_{320}$. The bars: 20 m (a to c) and 1 m (a-1 to c-2).*

Table 1. *The PMAA-b-P(iPMA-r-MAA) diblock copolymer by the polymrtiztion-induced self-assembly using the photo-NMP.*

DP of PMAA	iPMA (mmol)	MAA (mmol)	Time (h)	Conversion (%)		P(iPMA-*r*-MAA) block		M_n	M_w/M_n	Morphology	D_n (μm)	D_w/D_n
				iPMA	MAA	DP	iPMA/ MAA					
211	6.76	1.48	8	92	60	368	0.875/ 0.125	60,100	1.85	Sphere	5.24	2.30
211	5.59	2.65	8	80	55	306	0.755/ 0.245	47,800	1.68	Sphere	1.87	1.23
211	4.97	3.36	8	77	54	293	0.676/ 0.324	48,500	1.59	Sphere	3.65	2.99
211	4.28	3.95	8	78	61	298	0.583/ 0.417	64,000	1.52	Sheet	—	—
212	5.59	2.65	10	90	71	360	0.727/ 0.273	48,800	1.65	Sphere	1.44	1.14
216	6.90	2.38	14[a]	92	73	191	0.768/ 0.232	30,500	1.81	Sphere	1.53	1.20
239	9.32	2.94	14[a]	96	73	255	0.807/ 0.193	66,300	1.72	Sphere	1.04 0.274	2.37 1.21
244	12.4	3.91	14[b]	95	77	384	0.797/ 0.203	65,700	1.76	Sphere	2.46 0.299	1.39 1.27
244	3.59	3.31	14[a]	87	71	126	0.570/ 0.430	43,500	1.31	Sheet	—	—
250	6.90	6.38	14[a]	88	76	251	0.554/ 0.446	55,100	1.49	Sphere + Sheet	—	—
248	9.32	8.61	14[a]	92	78	350	0.562/ 0.438	84,900	1.48	IHP[c]	—	—

[PMAA]=4.83 mM, solvent: 4 mL.
[a] Solvent: 9 mL. [b] Solvent: 8 mL. [c] Inverted hexagonal phase.

Furthermore, the short block with a low iPMA ratio provided a sheet-like morphology consisting of unspecific nanoparticles. As shown in Figure 6, the sheets were transformed into spherical vesicles and flexible sheets and finally into aggregates with hollow tubes by extending the hydrophobic chain length. Detailed observations revealed that the aggregates had an inverted hexagonal phase [24] reticularly perforated (Figure 7). The nPMA-copolymer produced flexible sheets with a smooth surface without any pores. The linear propyl chains form the dense surface due to the more packed hydrophobic phase. On the other hand, the MMA-substituted copolymer provided rods of laminated sheets. It was found that the formation of the inverted hexagonal phase by the iPMA copolymer was due to the spatial thinness based on the steric repulsion of the bulky isopropyl groups.

In future work, we will create vesicles with the hydrophobic hexagonal phase that is nanoporous and permeable to gas, water, and ions.

4. Conclusion

The morphology of vesicles consisting of the iPMA-containing diblock copolymer was closely related not only to the hydrophobicity of the iPMA but also to the bulky isopropyl group. The copolymer with a very high iPMA ratio produced large spherical vesicles due to expansion of the internal hydrophobic phase by the bulky isopropyl groups. By decreasing the iPMA ratio, the vesicles shrank due to the predominance of intramolecular hydrogen bonding between the MAA unis over the steric repulsion of the isopropyl groups. A further decrease in the iPMA ratio expanded the vesicles again due to an increase in the hydrophilicity of the hydrophobic block. The copolymer with a still lower iPMA ratio produced a sheet-like morphology. The morphology was also manipulated by the chain length of the hydrophobic block for the iPMA ratio constant. At a high iPMA ratio, the copolymer with a short hydrophobic block produced micron-sized spherical vesicles embedded in the unspecific nanoparticle domain. By extending the block length, the unspecific nanoparticles grew into micron-sized spherical vesicles. On the other hand, the copolymer with the short block formed a sheet-like morphology at a low iPMA ratio. As a result of extending the block length, the sheets were transformed into aggregates with an inverted hexagonal phase that was formed by the steric repulsion of the isopropyl groups. These findings indicate that the morphology of the vesicles is manipulated not only by the hydrophobicity of the copolymer, but also by the bulkiness of the branched side chain in the hydrophobic block.

Conflict of Interest

The author has no conflict of interest in this study.

Acknowledgements

This study was supported by the JSPS Grant-in-Aid for Scientific Research (Grant Number 18K04863).

References

[1] Sadava, D. E. (1993). Cell Biology: Organelle structure and function, John and Bartlett, Boston.

[2] Tanford, C. (1980). The Hydrophobic Effect: Formation of micelles and biological membranes, 2nd Ed., Wiley-Interscience, New York.

[3] Campbell, M., Naworal, J. (1969). Composition of the saturated and monounsaturated fatty acids of Mycobacterium phlei. Journal of Lipid Research, 10, 593-598.

[4] Clejan, S., Krulwich, T. A., Mondrus, K. R., Seto-Young, D. (1986). Membrane lipid composition of obligately and facultatively alkalophilic strains of Bacillus spp. Journal of Bacteriology, 168, 334-340.

[5] Kyte, J., Doolittle, R. F. (1982). A simple method for displaying the hydropathic character of a protein. Journal of Molecular Biology, 157, 105-132.

[6] Černoch, P., Jager, A., Černochová, Z., Sincari, V., Albuquerque, L. J. C., Konefal, R., Pavlova, E., Giacomelli, F. C., Jager, E. (2021). Engineering of pH-triggered nanoplatforms based on novel poly (2-methyl-2-oxazoline)-*b*-poly[2-(diisopropylamino)ethyl methacrylate] diblock copolymers with tunable morphologies for biomedical applications. Polymer Chemistry, 12, 2868-2880.

[7] Wei, P., Cornel, E. J., Du, J. (2021). Breaking the corona symmetry of vesicles. Macromolecules, 54, 7603-7611.

[8] Yoshida, E. (2013). Giant vesicles prepared by nitroxide-mediated photo-controlled/living radical polymerization-induced self-assembly. Colloid and Polymer Science, 291, 2733-2739.

[9] Yoshida, E. (2015). Fabrication of microvillus-like structure by photopolymerization-induced self-assembly of an amphiphilic random block copolymer. Colloid and Polymer Science, 293, 1841-1845.

[10] Yoshida, E. (2019). Perforated giant vesicles composed of amphiphilic diblock copolymer: New artificial biomembrane model of nuclear envelope. Soft Matter, 15, 9849-9857.

[11] Yoshida, E. (2018). Morphology transformation of giant vesicles by a polyelectrolyte for an artificial model of a membrane protein for endocytosis. Colloid and Surface Science, 3 (1), 6-11.

[12] Yoshida, E. (2015). Morphological changes in polymer giant vesicles by intercalation of a segment copolymer as a sterol model in plasma membrane. Colloid and Polymer Science, 293, 1835-1840.

[13] Yoshida, E. (2014). Fission of giant vesicles accompanied by hydrophobic chain growth through polymerization-induced self-assembly. Colloid and Polymer Science, 292, 1463-1468.

[14] Yoshida, E. (2017). Fabrication of anastomosed tubular networks developed out of fenestrated sheets through thermo responsiveness of polymer giant vesicles. Chem Xpress, 10 (1), 118, 1-11.

[15] Yoshida, E. (2015). PH response behavior of giant vesicles comprised of amphiphilic poly(methacrylic acid)-*block*-poly(methyl methacrylate-*random*-methacrylic acid). Colloid and Polymer Science, 293, 649-653.

[16] Yoshida, E. (2015). Enhanced permeability of Rhodamine B into bilayers comprised of amphiphilic random block copolymers by incorporation of ionic segments in the hydrophobic chains. Colloid and Polymer Science, 293, 2437-2443.

[17] Yoshida, E. (2014). Morphology control of giant vesicles by manipulating hydrophobic-hydrophilic balance of amphiphilic random block copolymers through polymerization-induced self-assembly. Colloid and Polymer Science, 292, 763-769.

[18] Kobayashi, S., Uyama, H., Yamamoto, I., Matsumoto, Y. (1990). Preparation of monodispersed poly(methyl methacrylate) particle in the size of micron range. Polymer Journal, 22, 759-761.

[19] Miyazawa, T., Endo, T., Shiihashi, S., Ogawara, M. (1985). Selective oxidation of alcohols by oxoaminium salts (R2N:O+ X-). The Journal of Organic Chemistry, 50, 1332-1334.

[20] Yoshida, E. (2012). Effects of illuminance and heat rays on photo-controlled/living radical polymerization mediated by 4-methoxy-2,2,6,6-tetramethylpiperidine-1-oxyl. ISRN Polymer Science, 102186.

[21] Yoshida, E. (2010). Nitroxide-mediated photo-living radical polymerization of methyl methacrylate using (4-*tert*-butylphenyl)diphenylsulfonium triflate as a photo-acid generator. Colloid and Polymer Science, 288, 239-243.

[22] Yoshida, E. (2013). Nitroxide-mediated photo-controlled/living radical polymerization of methacrylic acid. Open Journal of Polymer Chemistry, 3, 16-22.

[23] Yoshida, E. (2014). Hydrophobic energy estimation for giant vesicle formation by amphiphilic poly(methacrylic acid)-*block*-poly(alkyl methacrylate-*random*-methacrylic acid) random block copolymers. Colloid and Polymer Science, 292, 2555-2561.

[24] Israelachvili, J. N. (2011). Intermolecular and Surface Forces, 3rd ed. Academic Press, Waltham.